arXiv:1206.0030v1 [astro-ph.SR] 31 May 2012

MECHANISMS FOR MHD POYNTING FLUX GENERATION IN SIMULATIONS OF SOLAR PHOTOSPHERIC MAGNETO-CONVECTION

S. Shelyag, M. Mathioudakis, F.P. Keenan
Astrophysics Research Centre, School of Mathematics and Physics, Queen's University, Belfast, BT7 1NN, Northern Ireland, UK
(Dated: 01.01.01/01.01.01)
Draft version June 4, 2012

ABSTRACT

We investigate the generation mechanisms of MHD Poynting flux in the magnetised solar photosphere. Using radiative MHD modelling of the solar photosphere with initial magnetic configurations that differ in their field strength and geometry, we show the presence of two different mechanisms for MHD Poynting flux generation in simulations of solar photospheric magneto-convection. The weaker mechanism is connected to vertical transport of weak horizontal magnetic fields in the convectively stable layers of the upper photosphere, while the stronger is the production of Poynting flux in strongly magnetised intergranular lanes experiencing horizontal vortex motions. These mechanisms may be responsible for the energy transport from the solar convection zone to the higher layers of the solar atmosphere.

Subject headings: Sun: Photosphere — Sun: Surface magnetism — Plasmas — Magnetohydrodynamics (MHD)

1. INTRODUCTION

The magnetic coupling between the solar interior and the outer layers of the solar atmosphere plays a key role in the energy transport between these regions. We have recently demonstrated (Shelyag et al. 2011a) that vorticity generation in the intergranular lanes of magnetic solar plage region simulations is much more efficient compared to the non-magnetic case. These vortices have been detected in observations of the photosphere and chromosphere (see e.g. Bonet et al. 2008; Wedemeyer-Böhm & Rouppe van der Voort 2009). The magnetic vortex motions are highly significant as they can deposit large amounts of energy in the solar chromosphere (Moll et al. 2012), contribute to the production of Poynting flux and generate various types of MHD wave modes (Shelyag et al. 2011b; Fedun et al. 2011). On the other hand, using a simulation setup that involved influx of weak horizontal magnetic field through the bottom boundary of the simulation domain, Steiner et al. (2008) have shown that the Poynting flux is generated through the advection of horizontal magnetic fields by vertical upflows in the upper, convectively stable layers of the solar photosphere. Abbett & Fisher (2012) have recently demonstrated the presence of Poynting flux in their radiative MHD simulations of an open-flux region of the solar atmosphere.

In this paper we use forward modelling techniques to examine the generation of Poynting flux in a model of the solar magneto-convection with different initial magnetic field strengths and geometries. Our model includes the wavelength-dependent radiative transport and the partial ionisation of a plasma with solar chemical composition. We perform simulation runs with initial vertical magnetic fields of 10 G and 200 G, as well as with changing polarity with unsigned flux of 200 G and with weak horizontal magnetic field of 10 G, advected into the numerical domain by convective upflows. The effectiveness of Poynting flux generation is analysed in these simulations and we find that Poynting flux generation by vortices, outlined by Shelyag et al. (2011b), is more pronounced irrespective of the magnetic configuration. We use a mixed-polarity region to study the dependence of Poynting flux generation relative to the degradation of activity.

2. SIMULATION SETUP

Our numerical modelling of the solar magnetised photosphere is undertaken using the MURaM radiative MHD code (Vögler et al. 2005). The code is described in detail in Vögler (2003) and it has been successfully used for a wide variety of applications in solar physics. Here we provide only a brief description of the code. It uses 4-th order central difference operators to calculate spatial derivatives, a 4-th order Runge-Kutta scheme to advance the solution in time, and hyperdiffusive operators to stabilise the solution against numerical instabilities. A non-grey radiative source term is included in the MHD equations to account for wavelength-dependent radiative energy exchange in the simulated photosphere, and a non-ideal equation of state is used, which takes into account partial ionisation of the 11 most abundant elements in the solar photosphere. Side boundary conditions are periodic, and the top boundary is closed for in- and outflows, while allowing horizontal motions of fluid and magnetic field lines. The bottom boundary condition is open for in- and outflows. In the simulations with an initial vertical magnetic field, magnetic field lines are forced to be vertical at the bottom boundary. We also use an alternative configuration of the bottom boundary condition, that allows the influx of horizontal magnetic field with a strength of 10 G in the convective upflow regions and leaves the outflows unaffected. This configuration has been described in more detail by Stein & Nordlund (2006) and has been used in the simulations of Steiner et al. (2008).

We use a domain size of 12×12 Mm^2 in the horizontal directions, and 1.4 Mm in the vertical, resolved by 480×480 and 100 grid cells, respectively. The domain
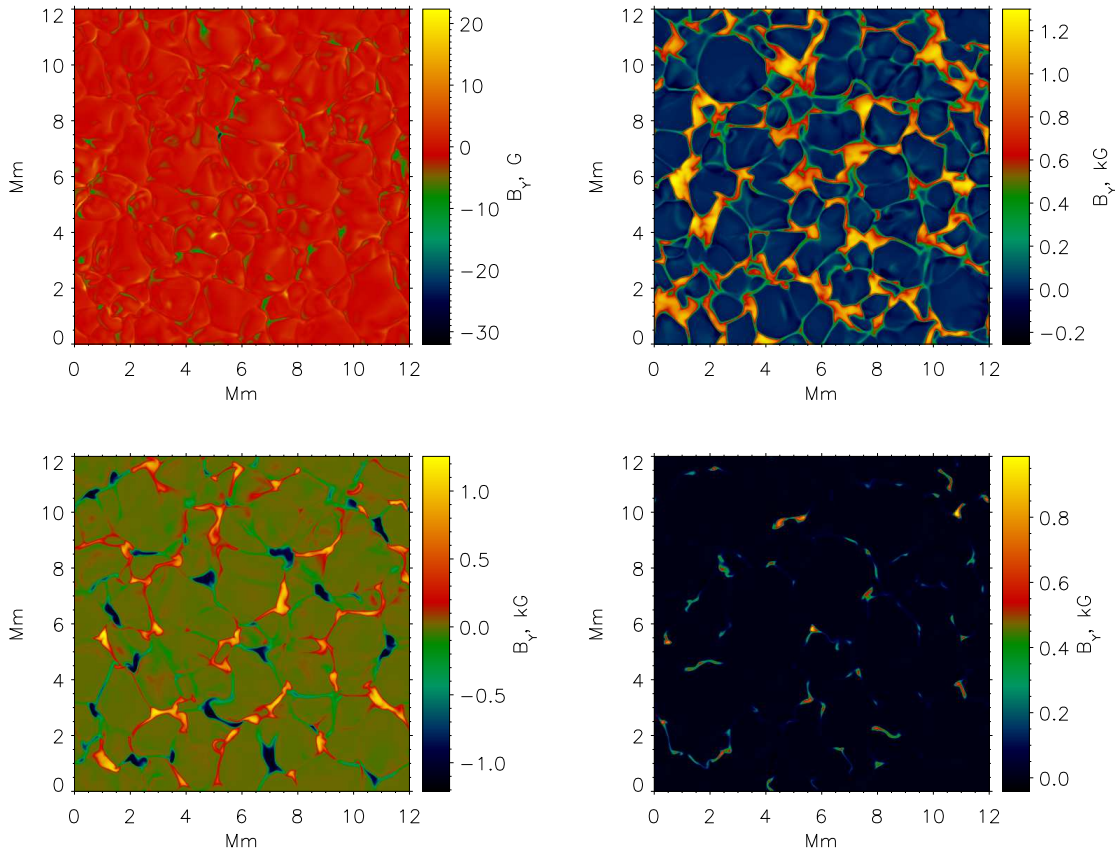
FIG. 1.— Vertical component of the magnetic field measured at the photospheric level in four simulations that differ in their initial field strength and geometry. Top left: horizontal magnetic field of 10 G advected through the bottom boundary of the numerical domain; top right: 200 G initial vertical magnetic field; bottom left: mixed-polarity initial vertical 200 G magnetic field, bottom right: 10 G initial vertical magnetic field simulation. The images have been taken approximately 800 s after the magnetic field was introduced into the domain.

is positioned in such way that the continuum formation level is located approximately 800 km above the bottom boundary. We use this setup to perform a series of simulations with 10 G and 200 G initial uniform vertical magnetic fields, as well as a simulation with initial vertical magnetic field of mixed (positive-negative) polarity with a net strength of 200 G, similar to that used by Cameron et al. (2011). A simulation with a 10 G horizontal magnetic field, advected with upflows into the domain though its bottom boundary, is also carried out.

Starting from a non-magnetic photospheric convection snapshot, we introduced these magnetic fields and boundary conditions in the domain and recorded sequences of magneto-convection snapshots over a few granular lifetimes.

In Fig. 1, vertical magnetic field distribution $B_y(x,z)$ in the domain at the photospheric level is shown for four simulation runs of different field strength and geometry. The top left panel shows that the interaction of horizontal magnetic field influx with convective flows does not form strong intergranular magnetic flux concentrations, in contrast to the 10 G and 200 G initial vertical uniform magnetic field (top right and bottom right). Small-scale loop-like structures with magnetic fields of about $10-30$ G are formed instead due to the advection of magnetic field by granular upflows. The area covered by magnetic field concentrations in the 10 G vertical case is significantly lower compared to that for 200 G,

and the magnetic field strength in these concentrations is also somewhat lower. In the bottom left panel of Fig. 1 the distribution of the vertical component of magnetic field for the mixed-polarity simulation is shown. Here, strong magnetic flux concentrations with strengths of up to about 1.2 kG are initially formed. However, the net magnetic flux decreases during the simulation as a result of opposite-polarity magnetic flux reconnection and cancellation (Cameron et al. 2011), and due to the magnetic diffusivity in this relatively low-resolution run. (See e.g. Vögler & Schüssler 2007, for a discussion of magnetic field generation and decay speed dependence on the numerical grid resolution and effective magnetic Reynolds number).

The 10 G initial vertical uniform magnetic field and 10 G horizontal magnetic field simulations show significant differences in the evolution of their average quantities. This is plotted in Fig. 2, where the time evolution of the modulus of horizontal components of magnetic field is shown for the two cases. In the horizontal magnetic field simulation, it takes approximately 15 minutes for the magnetic field to propagate from the bottom boundary of the domain to the photospheric level (marked by $y = 0$ in the left plot of Fig. 2). In agreement with the findings of Steiner et al. (2008), the horizontal magnetic field is accumulated at a height of approximately 0.15 Mm above the average continuum formation level $y = 0$. This is visible as a small increase in the average
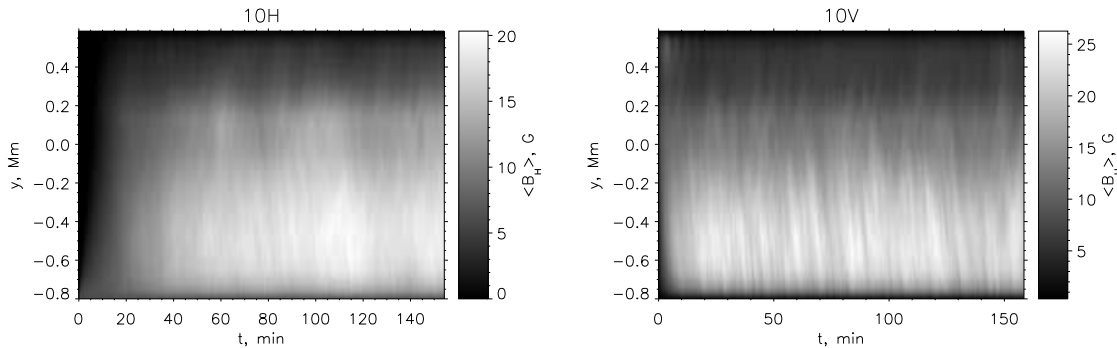
FIG. 2.— Time evolution of average horizontal magnetic field strength as a function of height. Left panel: 10 G horizontal magnetic field advected through the bottom boundary; right panel: a 10 G initially vertical magnetic field simulation.
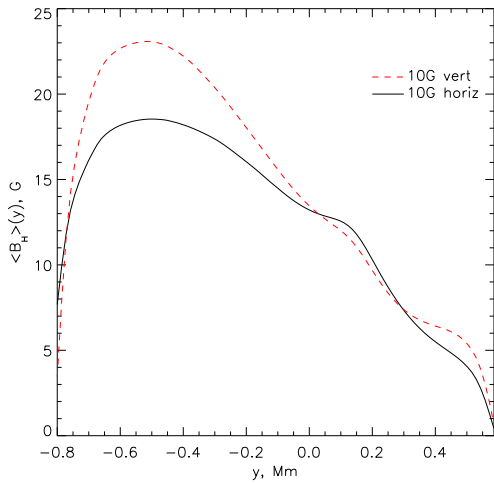

FIG. 3.— Time average of the variation in the mean horizontal magnetic field with height. The dashed curve corresponds to the 10 G initial vertical uniform magnetic field setup, while the black solid curve is the 10 G horizontal magnetic field simulation.

horizontal magnetic field at this height. A similar plot for the 10 G vertical field is shown in the right panel of Fig. 2. In the latter case, the vertical magnetic field is redistributed by the convective flows within the first 5 minutes of the simulation, and the horizontal component of the magnetic field appears. There is also no clear layer where the horizontal magnetic field is accumulated. This is further demonstrated in Fig. 3, where we plot the time averages of the dependence of the horizontal magnetic field as a function of height. The figure shows a local enhancement of the horizontal magnetic field strength at $y = 0.15$ Mm for 10 G horizontal field simulation, while for the vertical magnetic field simulation there is almost no enhancement.

3. POYNTING FLUX ANALYSIS

We define the MHD Poynting flux vector as

$$\mathbf{F} = \frac{1}{4\pi}\mathbf{B} \times (\mathbf{v} \times \mathbf{B}),\qquad(1)$$

where $\mathbf{B}$ is the magnetic field vector and $\mathbf{v}$ is velocity field vector. We are interested in the vertical component of the Poynting flux vector F_y (note that, in our notation, the y vector component corresponds to the vertical, while x and z correspond to the horizontal directions) which is

defined as

$$F_y = \frac{1}{4\pi}\left(v_y\left(B_x^2 + B_z^2\right) - B_y\left(v_x B_x + v_z B_z\right)\right) = F_y^{\mathrm{v}} + F_y^{h}.\qquad(2)$$

In Eq. (2), F_y^{v} corresponds to the part of the vertical component of the Poynting flux vector produced by vertical motions, and represents the transport of horizontal magnetic field with vertical velocity, while F_y^{h} is the part of the vertical component, generated by horizontal magnetised plasma motions.

The F_y, F_y^{v} and F_y^{h} components of the Poynting flux vector for 10 G vertical and 10 G horizontal magnetic field simulations, measured at 500 km height above the average continuum formation level in the simulation domain, are shown in the left, middle and right panels of Fig. 4, respectively. For both simulations, the total vertical (y) component of Poynting flux is generally positive. A positive vertical Poynting flux is therefore a general property of the simulated photosphere and does not depend on the initial magnetic field geometry. However, our simulations show that the average F_y is about 10 times smaller for the case of horizontal magnetic field compared to the 10 G initial vertical magnetic field. This finding holds for the latest stages of the simulation which have achieved a state of equilibrium.

The middle panel of Fig. 4 shows the amount of the vertical Poynting flux, generated by the vertical motions. It is evident from the plot that the horizontal magnetic field simulation produces an average vertical Poynting flux which is positive, while the vertical magnetic field does not. This confirms the presence of the mechanism of vertical Poynting flux production by advection of horizontal magnetic field in the upward direction, as described by Steiner et al. (2008). However, as shown in the right panel of Fig. 4, only about 5% of the total vertical Poynting flux is produced by the upward advection of horizontal magnetic fields. This comparison clearly shows that it is the strong vertical magnetic fields in the upper photosphere that are mainly responsible for the vertical Poynting flux production. As previously shown by Shelyag et al. (2011b), this flux is produced by the interaction of vortex flows in the intergranular lanes with the expanding photospheric magnetic concentrations. The positive sign (outward direction) of Poynting flux is not connected either to the initial magnetic field direction, or to the way the magnetic field is introduced into the domain. To demonstrate this further, in Fig. 5 we compare the Poynting flux produced with an initial positive
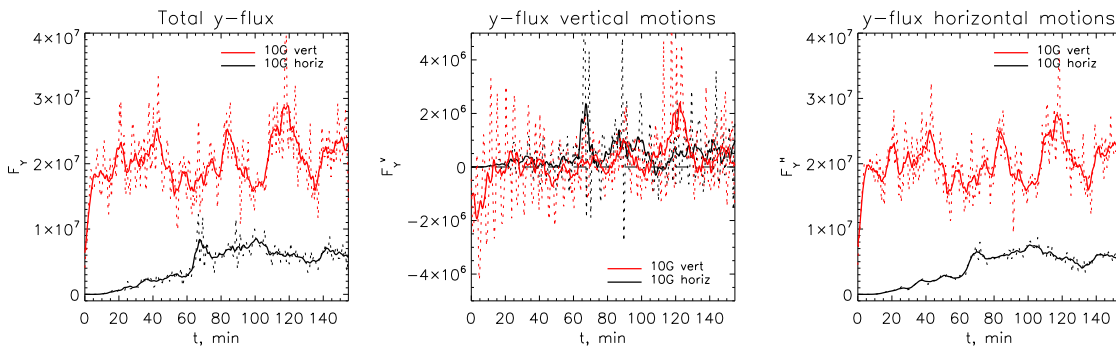
FIG. 4.— The time dependence of the total vertical Poynting flux (left) and its components F_y^v (middle) and F_y^h (right) for the 10 G vertical (red) and 10 G horizontal simulations. Solid lines in the plots correspond to the time dependences, obtained by smoothing with a boxcar window of width 5 minutes, while dotted lines are the non-smoothed dependences. Note that the fluxes for the 10 G horizontal magnetic field simulations are multiplied by a factor of 5 to allow their comparison with the 10 G vertical simulations.
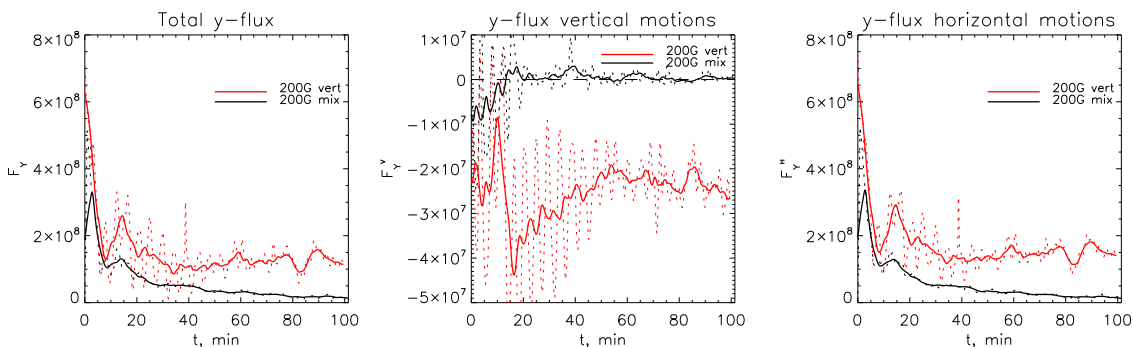

FIG. 5.— Same as Fig. 2 for 200 G initial vertical and 200 G initial mixed polarity magnetic field simulations.

vertical 200 G field with that of a mixed-polarity vertical 200 G field. The dependence of the total vertical component of the Poynting flux with time (left panel of Fig. 5) shows that after the first 5 minutes, during which the magnetic field is advected into the intergranular lanes, the behaviour of the vertical magnetic field simulation stabilises, while the flux emerging from the mixed-polarity simulation begins to decay. In contrast to the weaker, 10 G vertical uniform field simulation, the vertical Poynting flux generated by vertical motions is now negative, suggesting larger amount of stronger horizontal fields located in the vertical downflow regions. During the first 20 minutes of the simulation, the mixed-polarity model also shows a negative Poynting flux produced by vertical motions (middle panel of Fig. 5). However, after this stage, when a significant amount of vertical magnetic field has cancelled out, the horizontal small-scale magnetic loop-like structures in the granular upflow regions (Cameron et al. 2011) start producing positive Poynting flux, similar to the 10 G horizontal field model. As the right panel of Fig. 5 shows, both models generate vertical positive Poynting flux due to horizontal motions in strong vertical magnetic field concentrations, which is about two orders of magnitude larger than the Poynting flux produced by vertical motions.

It has to be noted that the height of 500 km for the measurement of the Poynting flux has been chosen arbitrarily. The results presented remain valid everywhere where the Poynting flux is positive, far away from the upper boundary and in a wide range of heights starting from about 200 km above the photospheric level. Thus,

the influence of the upper boundary condition is considered to be small on these measurements.

In general, the 10 G simulations show notably more turbulent behaviour of Poynting flux compared to the 200 G models. While the latter shows the oscillations in F_y, the former demonstrates a more random dependence of F_y with time. This is due to the presence of a large relative amount of weak, turbulent granular fields compared to the strong magnetic field model, where the major part of magnetic flux is concentrated in the intergranular lanes.

It is also interesting to note that the Poynting flux in the vertical direction does not scale simply as the square of the magnetic field strength, as may be suggested from Eq. (2). While the ratio of squares of the mean magnetic field in the 10 and 200 G simulations is 400, the ratio of the average vertical Poynting fluxes in these models is about 10. This is due to the magnetic field in the intergranular lanes, which does not increase linearly with increasing initial field. However, it tends to occupy a larger area of the intergranular lanes, thus increasing the filling factor. This process continues until the intergranular lanes are fully filled with the magnetic field. Any further increases in the initial magnetic field strength lead to the appearance of a dynamically different sunspot umbra region (Schüssler & Vögler 2006).

4. CONCLUSIONS

In this paper we carried out a comparative analysis of the Poynting flux generated by simulated magnetised solar photospheres with magnetic fields that differ in

strength and geometry. We have shown the presence of two different types of vertical Poynting flux generation: one connected to the advection of horizontal magnetic field by upflows in the photosphere, while the other is due to horizontal motions of plasma in strong intergranular magnetic flux concentrations. Using different initial magnetic field strength photospheric magneto-convection simulations, mixed polarity region simulations and simulations with the horizontal magnetic field advected through the bottom domain boundary, we showed that the latter mechanism is the preferred one, independent of both how the magnetic field is introduced in the simulated photosphere, and the direction of initial magnetic field. We demonstrated clearly that the outward flux of electromagnetic energy (Poynting flux) is a general property of the simulated photosphere and does not depend on the way how the magnetic field is introduced in the domain.

The initial magnetic field configurations presented in this paper can be related to regions of the solar photosphere. Our weak magnetic field (10 G) simulations correspond to a case of an extremely weakly magnetised solar granulation, while the 200 G uniform and opposite-polarity models allow production of stronger horizontal fields and represent the evolution of unipolar or bipolar regions in proximity to sunspots. The results shown suggest that both magnetically active and non-active granulation deliver electromagnetic energy to the upper layers of solar atmosphere. While simulated active regions with strong vertical magnetic fields generate 5 times more Poynting flux compared to non-active regions, the area covered by non-magnetic granulation can be significantly larger than the one covered by active regions, depending on the global solar activity level.

REFERENCES

Abbett, W. P., & Fisher, G. H. 2012, Sol. Phys., 277, 3
Bonet, J. A., Márquez, I., Sánchez Almeida, J., Cabello, I., & Domingo, V. 2008, ApJ, 687, L131
Cameron, R., Vögler, A., & Schüssler, M. 2011, A&A, 533, A86
Jess, D. B., Mathioudakis, M., Christian, D. J., Keenan, F. P., Ryans, R. S. I., & Crockett, P. J. 2010, Sol. Phys., 261, 363
Fedun, V., Shelyag, S., Verth, G., Mathioudakis, M., & Erdélyi, R. 2011, Annales Geophysicae, 29, 1029
Moll, R., Cameron, R. H., & Schüssler, M. 2012, arXiv:1201.5981
Schüssler, M., & Vögler, A. 2006, ApJ, 641, L73
Shelyag, S., Schüssler, M., Solanki, S. K., Berdyugina, S. V., Vögler, A. 2004, A&A, 427, 335
Shelyag, S., Schüssler, M., Solanki, S. K., Vögler, A. 2007, A&A, 469, 731
Shelyag, S., Keys, P., Mathioudakis, M., & Keenan, F. P. 2011, A&A, 526, A5
Shelyag, S., Fedun, V., Keenan, F. P., Erdélyi, R., & Mathioudakis, M. 2011, Annales Geophysicae, 29, 883
Stein, R. F., & Nordlund, Å. 2006, ApJ, 642, 1246
Steiner, O., Rezaei, R., Schaffenberger, W., & Wedemeyer-Böhm, S. 2008, ApJ, 680, L85
Vögler, A., Shelyag, S., Schüssler, M., Cattaneo, F., Emonet, T., & Linde, T. 2005, A&A, 429, 335
Vögler, A. 2003, PhD thesis, University of Göttingen, Germany, http://webdoc.sub.gwdg.de/diss/2004/voegler
Vögler, A., & Schüssler, M. 2007, A&A, 465, L43
Wedemeyer-Böhm, S., & Rouppe van der Voort, L. 2009, A&A, 507, L9